J. Webster (ed.), *Wiley Encyclopedia of Electrical and Electronics Engineering*

RADAR TARGET RECOGNITION

Recent advances in radar provide sufficient resolution and enough information to recognize tactical targets from radar returns (1). For target recognition applications, different types of radar, such as synthetic aperture radar (*SAR*), millimeter wave (*MMW*) real aperture radar (*RAR*), and interferometric synthetic aperture radar (*IFSAR*), have been explored. Modern radar systems also provide extensive data, including fully polarimetric and Doppler channels, but there still are many challenges for target recognition using radar returns. The special characteristics of radar and recent advances in radar technology make the recognition of targets difficult. For example, the radar profile changes drastically for a small change in look angle, and the recent development of stealth technology significantly alters the radar signature. This article covers many of the different approaches for different radar types of radar target recognition.

Synthetic aperture radar provides high resolutions for both range and azimuth directions and has been used widely for target recognition applications. Since SAR is an imaging radar, it can provide detailed images of target areas with cloud-penetrating characteristics. When its fully polarimetric data are utilized, targets can be recognized with high accuracy. The SAR target recognition is typically done in multiple stages (2). The first stage of a typical SAR target recognition algorithm is a prescreener, where regions of interest are located. A constant false-alarm rate (*CFAR*) detection algorithm is often used in the first stage. The second stage may be a discriminator, where natural clutter false alarms are rejected. In this stage, textural features are extracted from the target-size windows applied to the neighborhood of pixels located by CFAR detection. The third stage is typically a classifier, where the targets are classified and human-made discretes are rejected. Extensive studies in statistical pattern recognition have been done, and many different pattern classifiers are used in target recognition applications. For SAR target recognition, spatial matched filters are investigated (2) for the recognition of ground vehicles. Novak's (2) spatial matched filter approach in target recognition is explained in later sections.

Although SAR technology provides many advantages over RAR there are many applications for which RAR is important. The azimuth resolution of SAR is much better than that of RAR, but it is typically based on the assumption that the movement of the radar is at constant speed and direction. When the radar is moving at a rapidly changing speed and trajectory, as in the case of the radar mounted on fighter airplanes or self-guided weapons, the assumptions for SAR processing are not correct. Millimeter wave RAR represents the next generation of military smart sensors for detection, tracking, and surveillance due to its high-range resolution, which is critical in target recognition. The MMW RAR technology is sufficiently advanced, and the range resolution of MMW radar is sufficiently high to discriminate tactical targets at a distance of several kilometers (3). The target recognition by hierarchical modeling of high-range resolution (*HRR*) MMW radar signatures is discussed in this article.

Artificial neural networks (*ANN*) have been widely used in target recognition. The use of ANN in radar target recognition is also discussed in this article. ANNs are used as pattern classifiers and feature extractors and in model adaptation and fuzzy classification in radar target classification. Feed-forward neural networks have been used as pattern classifiers after being "trained" with known target samples. The leaning algorithm of neural networks provides a powerful tool for adaptation of the classifier to input vectors (4). A self-organizing

feature map (*SOM*) has been used as a feature extractor (5) for radar target recognition. In combination with Kohonen's learning vector quantizer (*LVQ*) for supervised classification, SOM has been applied to the recognition of ground vehicles from MMW HRR radar signatures (5). Perlovsky, et al. (6) suggested the model-based neural network to include a priori information to an ANN. This approach can reduce the search space of the neural network by incorporating a priori information to the adaptability of an ANN. The fuzzy neural network approach (7) is also suggested to classify targets that may belong to more than one class. The advances in neural network approaches can improve the performance of target recognition algorithms further. There are many approaches to incorporating information from many different sources for radar target recognition. By fusing the information from more than one sensor, the accuracy of radar target recognition may be improved. Two approaches in utilizing information from multiple sensors are discussed in this article. IFSAR provides elevation information, in addition to two-dimensional radar images, by processing interference between radar returns received by two different antennas. By processing IFSAR images and fusing to SAR of visual images, the accuracy of the target recognition can be improved substantially. The approach of combining IFSAR and visual images using image registration approach is discussed in this article. There are statistical approaches in data fusion, and Bayesian data fusion approaches are used in radar target recognition (8). In this approach, features from polarimetric SAR images are fused to improve the recognition accuracy.

Radar target recognition is a complex problem, and no single algorithm performs better than other algorithms with different types and modes of radar. In this article, different approaches for radar target recognition are discussed in terms of radar types and approaches.

Hierarchical Modeling Approach for Noncooperative Target Recognition

Target recognition using hierarchical modeling of MMW RAR radar signatures is considered in (9), and the algorithm is tested with MMW radar data from a noncooperative target identification (*NCTI*) database. In radar target recognition problems, the targets may be shifted and scaled from the trained data. The change in look angle results in a scale change in radar signature, and the change in azimuth angle results in a shifting of radar signature. Therefore, a classifier using features extracted from the radar signatures should classify targets reliably even when radar signatures are shifted or scaled. In general, parameters of time series models such as ARMA models are not scale invariant. Thus, the classification of scaled targets with model parameter features can result in poor classification accuracy. There are a few approaches to make a classifier more reliable to shifting and scaling. For example, the use of scale invariant features or a training with scaled samples can make a classifier more robust to scaling.

The hierarchical ARMA modeling approach is briefly discussed in the following. Suppose that a continuous signal $x(t)$ is a training sample. The classifier needs to classify the scaled signal of $x(t)$ correctly as the same class as $x(t)$. The scaled signal of $x(t)$ is given by

$$y_\alpha(t) = \frac{1}{\alpha} x(\alpha t) \qquad (1)$$

One approach to achieve this is to train a classifier with features extracted from scaled signals of $x(t)$. For example, different features at m different scales are extracted from scaled signals $y_{\alpha 1}(t), y_{\alpha 2}(t), \ldots, y_{\alpha m}(t)$; then the classifier is trained with these multiscale features. If the number of scales included in the training is large enough, the classifier will classify signals having large-scale changes.

However, there are at least two potential problems with this approach if the signal is a discrete signal $\{x(i), i = 1, \ldots, N\}$. First, the original signal is defined only at discrete points, and the signal at the finer scale is not defined at certain points. Second, feature extraction is performed multiple times with a single training sample,

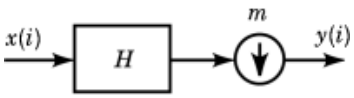

Fig. 1. A decimation filter.

and the computational complexity increases linearly as the number of scales increases. These difficulties can be solved by the hierarchical modeling approach. The hierarchical modeling approach presented in this section extracts multiscale features without adding much computational complexity.

A discrete signal can be scaled to a coarser scale or a finer scale by decimation filtering or interpolation, respectively. We will first consider the decimation filtering of a signal and its effect on the statistical model, and then we will consider the scaling to a finer scale as a modeling process. A decimation filter is defined as a local averaging (finite impulse response [*FIR*] filtering) followed by a down-sampling process, as shown in Fig. 1. If the down-sampling rate is m, the decimation-filtered signal represents the signal at the scale reduced by the factor of m. Let H be a FIR filter of length r and $\downarrow$ be the down-sampling operator of factor m.

$$H(\delta) = \sum_{k=0}^{r-1} h_k \delta^k, \text{ where } \delta \text{ is a unit delay operator} \qquad (2)$$

$$(\downarrow x)(i) = x(mi) \qquad (3)$$

Suppose that a signal at a coarser scale $y_m(i)$ is obtained by decimation-filtering of the original signal $x(i)$.

$$y_m(i) = H(\delta)x(im), \quad i = 1, \ldots, N/m \qquad (4)$$

Suppose that the signal $\{x(i), i = 1, \ldots, N\}$ follows an ARMA(p,q) model.

$$x(i) = \sum_{j=1}^{p} a_j x(i-j) + \sum_{j=0}^{q} b_j w(j), \quad i = 1, \ldots, N \qquad (5)$$

where $\{w(i)\}$ is a zero mean white noise sequence with variance $\sigma^2{}_w$, and a_j's and b_j's are real coefficients. Equation (5) can be rewritten as

$$A_p(\delta)x(i) = B_q(\delta)w(i), \quad i = 1, \ldots, N \qquad (6)$$

where

$$\begin{aligned} A_p(\delta) &= 1 - a_1\delta^1 - a_2\delta^2 - \cdots - a_p\delta^p \quad \text{and} \\ B_q(\delta) &= 1 + b_1\delta^1 + b_2\delta^2 + \cdots + b_q\delta^q \end{aligned} \qquad (7)$$

and δ is the unit delay operator, and we assume that the roots of $A_p(\delta)$ and $B_q(\delta)$ lie inside of the unit circle for stability and invertability of the model.

To find features at coarser scale, the model at a coarser scale should be considered. The following theorem summarizes the results on the modeling of a decimation-filtered ARMA process.

The decimation-filtered process $\{y_m(i)\}$ defined in Eq. (4) follows an ARMA(p,$q*$) model, where the order of AR polynomial is p, the order of the MA polynomial is $q* = [(p(m-1)+r+q-1)/m]$, and the model parameters can be obtained from the model parameters of $x(i)$.

$$C_p(\delta)y_m(i) = D_{q^*}(\delta)v(i) \tag{8}$$

where

$$\begin{aligned} C_p(\delta) &= 1 - c_1\delta^1 - c_2\delta^2 - \cdots - c_p\delta^p \\ D_{q^*}(\delta) &= 1 + d_1\delta^1 + d_2\delta^2 - \cdots + d_{q^*}\delta^{q^*} \end{aligned} \tag{9}$$

Also, the AR polynomial $C_p(\delta)$ of aggregated data satisfies the following relation:

$$\begin{aligned} C_p(\delta) &= 1 - c_1\delta^1 - \cdots - c_p\delta^p \\ &= (1 - r_1^m\delta)(1 - r_2^m\delta)\cdots(1 - r_p^m\delta) \end{aligned} \tag{10}$$

where $r_1, \ldots, r_p$ are roots of $A_p(\delta)$.

The proof can be found in (9).

The ARMA model parameters are shift invariant because this model's parameters depend only on mean and correlations. Power spectral density can be estimated by using ARMA model parameters and is also shift invariant and provides features that are intuitively appealing. For example, spectral peaks or notches represent the presence or absence of a frequency component in the signal. For radar signal classification, ARMA power spectrum features at multiple scales are used. Power spectral density of an ARMA process can be estimated by an extended least squares (*ELS*) method.

Suppose that $x(i)$ is an ARMA(p,q) process and $w(i)$ is the input white sequence with variance σ^2 as defined in Eq. (5). Let $R_{xx}(k)$ be the autocorrelation functions of $x(i)$, and $R_{xw}(k)$ be the cross correlation between $x(i)$ and $w(i)$. The Yule–Walker equation for the ARMA process $x(i)$ is given by the following:

$$R_{xx}(k) = \begin{cases} \displaystyle\sum_{i=1}^{p} a_i R_{xx}(k-i) + \sum_{i=1}^{q} b_i R_{xw}(k-i), & k = 0, \ldots, q \\ \displaystyle\sum_{i=1}^{p} a_i R_{xx}(k-i), & k > q \end{cases} \tag{11}$$

The AR parameters are estimated by solving the above Yule–Walker equations. By using the estimated AR parameters, the MA component of $x(i)$ can be obtained by filtering AR component from $x(i)$.

$$\hat{x}_{ma}(i) = x(i) - \sum_{k=1}^{p} \hat{a}_k x(i-k) \tag{12}$$

The power spectral density of the ARMA process $x(t)$ is estimated from the correlations of $x_{ma}(t)$ and the AR parameters estimated by Yule–Walker equations. The ELS power spectrum estimation algorithm is summarized as follows.

ELS Spectrum Estimation Algorithm

Step 1: Compute sample correlations $R_{xx}(k)$ for $k = 0, \ldots, p+q$.

$$\hat{R}_{xx}(k) = \frac{1}{N-k} \sum_{i=1}^{N-k} x(i)x(i+k) \tag{13}$$

Step 2: Estimate AR parameters $a_1, \ldots, a_p$ by

$$\begin{bmatrix} \hat{a}_1 \\ \vdots \\ \hat{a}_p \end{bmatrix} = \begin{bmatrix} R_{xx}(q) & \cdots & R_{xx}(q+1-p) \\ \vdots & \ddots & \vdots \\ R_{xx}(q+p-1) & \cdots & R_{xx}(q) \end{bmatrix}^{-1} \cdot \begin{bmatrix} R_{xx}(q+1) \\ \vdots \\ R_{xx}(q+p) \end{bmatrix} \tag{14}$$

Step 3: Compute the sample correlation of MA component $x_{ma}(i)$ that is obtained by removing the AR component.

$$\hat{R}_{ma}(k) = R_{xx}(k) - \sum_{j=1}^{p} a_j R_{xx}(k-j) - \sum_{j=1}^{p} a_j R_{xx}(k+j) + \sum_{j=1}^{p} \sum_{l=1}^{p} a_j a_l R_{xx}(k-j+l), k = 0, \ldots, q \tag{15}$$

Step 4: Compute the ARMA power spectrum.

$$S_{xx}(\omega) = \frac{R_{ma}(0) + 2\sum_{k=1}^{q} R_{ma}(k)\cos(\omega k)}{\left\| 1 - \sum_{k=1}^{p} \hat{a}_k e^{-j\omega k} \right\|^2} \tag{16}$$

For each training sample $x(i)$, the models at the other scales (both coarser and finer scales) are obtained by the hierarchical modeling approach presented in the previous section. The model at a coarser scale is obtained using Theorem 1. The AR polynomial is obtained by Eq. (10), and the correlation of the signal at the coarse scale is obtained with a proper choice of smoothing filter H, such as a Gaussian filter. Thus, the spectral density of the signal at a coarser scale is obtained by the ELS algorithm. The model at a finer scale is obtained by the approach explained in step 2. The AR polynomial of the signal at a finer scale is obtained under no-hidden-periodicity assumption. The correlation function at a finer scale is obtained by disaggregation (9),

and the ARMA spectrum at a finer scale is obtained by the ELS estimation algorithm. The multiscale feature extraction algorithm is summarized as follows.

Multiscale Spectral Feature Extraction Algorithm:

Step 1: Each radar return is normalized to zero mean and unit variance by

$$\bar{x}(i) = \frac{(x(i) - \hat{m})}{\hat{\sigma}} \tag{17}$$

where $\hat{m}$ and $\hat{\sigma}^2$ are sample mean and sample variances of $x(i)$. M K-dimensional features from M scales (including coarser and finer scales) are obtained from the normalized radar returns by the following procedure.

Step 2: For each training sample, the AR parameters and correlations are estimated by the ELS algorithm. For $k = 0, 1, \ldots, K-1$, the power spectrum is estimated at $\omega = \pi k/K$. The logarithm of the power spectral density forms a K-dimensional feature vector.

Step 3: At each coarser scale, a feature vector is obtained by estimating the power spectrum using the ELS method, with model parameters obtained by the hierarchical modeling approach. The logarithm of the power spectral density forms a K-dimensional feature vector at a coarser scale. Feature vectors at multiple scales are obtained by repeating this step at coarser scales.

Step 4: At each finer scale, a feature vector is obtained by estimating the power spectrum using the ELS method, with model parameters obtained by the hierarchical modeling approach. This is repeated for other finer scales, and multiple K-dimensional feature vectors are obtained from the logarithm of the power spectral density.

Classification is done by a minimum distance classifier with multiple prototypes. In this approach, each training sample generates M prototypes corresponding to M scales. Therefore, if there are N training signals for each class, then NM prototypes will be available for each class. Let us assume that there are N_k prototypes $z_k^1, \ldots, z_{N_k}^k$ in the class $k \in \{1, \ldots, K\}$. For a test pattern $\boldsymbol{x}$, the distance to the class k is defined by

$$D_k = \min\{d(\mathbf{x}, \mathbf{z}_k^l)\} \tag{18}$$

where the intersample distance $d(\boldsymbol{x}, \boldsymbol{z})$ is the Eucledian distance between $\boldsymbol{x}$ and $\boldsymbol{z}$. The distance D_i is the smallest of the distances between $\boldsymbol{x}$ and each of the prototypes of the class k. The test pattern $\boldsymbol{x}$ is classified by the minimum distance decision rule: $\boldsymbol{x}$ is classified into class k if $D_k < D_i$ for all $i \neq k$.

In Ref. 9, the hierarchical model-based features are tested with NCTI data. Figure 2 shows a typical NCTI radar signature and estimated power spectral density. In Ref. 9, about 95% of classification accuracy is reported with 5000 MMW RAR radar signatures.

Neural Network Approaches

Neural networks have been widely used in radar target recognition applications (4,5,6,7). A good survey on the use of neural networks in target recognition can be found in Ref. 4. Neural network approaches have been popular because they have many promising qualities in target recognition applications. Neural networks have the capability for adaptation to additional targets and environments. The existence of powerful learning algorithms is one of the main strengths of the neural network approach (4). Neural networks also offer techniques

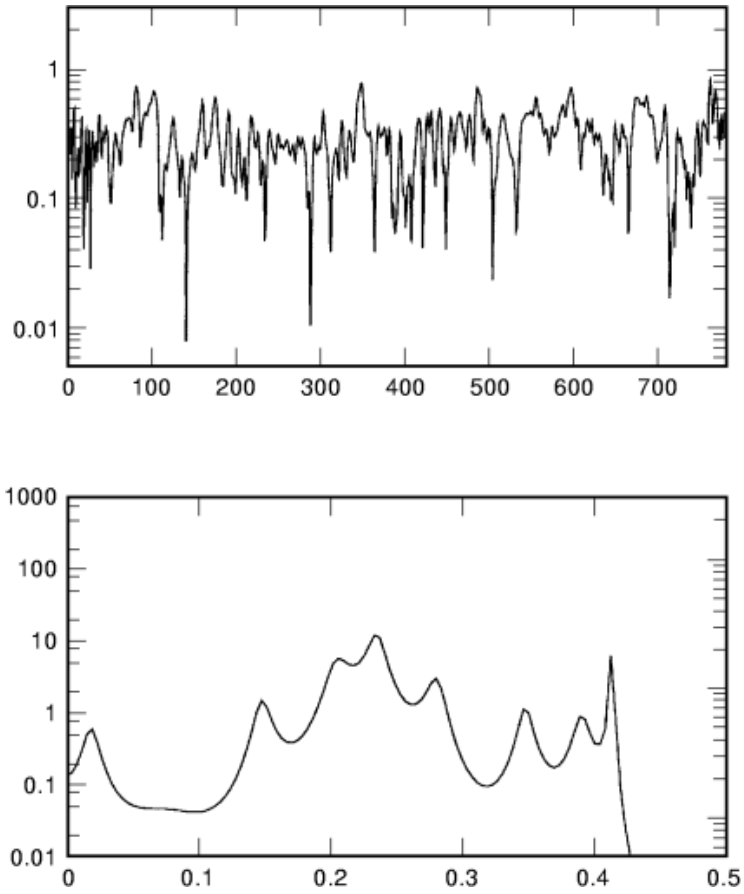

Fig. 2. A HRR radar signature from NCTI database and its power spectrum estimated by hierarchical modeling.

for selecting, developing, clustering, and compressing features into a useful set, and they provide automatic knowledge acquisition and integration techniques for target recognition systems.

Feed-forward neural networks have been used as a pattern classifier for the target recognition. (10). Let $\boldsymbol{x}_i$ be the multidimensional feature vector extracted from a radar image, and let S be the index set of the target patterns.

$$S = \{i | i \in \text{ target pattern}\} \tag{19}$$

The optimum receiver (10) defined by

$$R_s(x_1, \ldots, x_N) = \sum_{i \in S} x_i \tag{20}$$

can be implemented as a neural network:

$$y_s = \Theta\left(\sum_i W_{Si} x_i - T\right) \tag{21}$$

where T is the threshold and $\Theta(x)$ is the heavyside step function. Roth (10) showed that detection of target patterns out of a set of P of patterns can be handled by the preceding feed-forward neural network.

Neural networks have been also used as feature extractors for target recognition. Kohonen's self-organizing map (*SOM*) and LVQ have been used in the two-stage target recognition approach (5). SOM is based on unsupervised competitive learning where only one output node, or one per local group of nodes at a time, gives the active response to the current input signal, and it clusters input vectors into preselected C classes by adapting connection weights to nodes in the network, and is used as a feature extractor in Ref. 5. At each iteration of the SOM algorithm, the best matching node c is selected by

$$c = \text{argmin}\{\|\boldsymbol{x} - m_i\|\} \tag{22}$$

where $\boldsymbol{x}$ is the current input vector, and $\{m_1, \ldots, m_C\}$ is the set of nodes (cluster centers). Then each node m_i located in the neighborhood of the node c is adapted by the learning rule:

$$m_i(t+1) = m_i(t) + \eta_i(t)[x(t) - m_i(t)] \tag{23}$$

where the gain $\eta_i(t)$ can be a simple monotonically decreasing function of time or a Gaussian gain function defined by

$$\eta_i(t) = \alpha(t)\exp(-\|r_c - r_i\|^2)/(2\sigma^2(t)) \tag{24}$$

The learning rate $\alpha(t)$ and the kernel width $\sigma(t)$ are monotonically decreasing functions, and their exact forms are not critical. LVQ is used as a supervised classifier of the features extracted by SOM in Ref. 5. In Ref. 5, more than 94% of accuracy is reported in the target recognition experiment, with MMW data having five types of ground vehicles.

Recently, the model-based neural network (*MBNN*) was introduced (6) to combine a priori knowledge of models of data with adaptivity to changing data properties. The learning and adaptation of the MBNN is done by iterative estimation of association weights and model parameters. Different statistical models for different physical processes, background clutter, outlier, target pixels, and so on, are also introduced in Ref. 6. This approach has the potential to improve target recognition performances by allowing inclusion of a priori information in addition to the adaptability of a neural network.

Fuzzy neural networks are also used in radar target recognition. Fuzzy ARTMAP and EMAP neural networks are suggested (7) for radar target recognition. Fuzzy neural networks allow us to make soft decisions in classifying a target, and each input vector can belong to more than one class. The fuzzy association between the input vector and the classified target can improve the performance and the complexity of the adaptation.

Exploitation of Elevation Data from IFSAR

IFSAR is a technique to generate high-resolution digital elevation model (*DEM*) based on the phase difference in SAR signals received by two spatially separated antennas (11). There are drawbacks in height maps derived

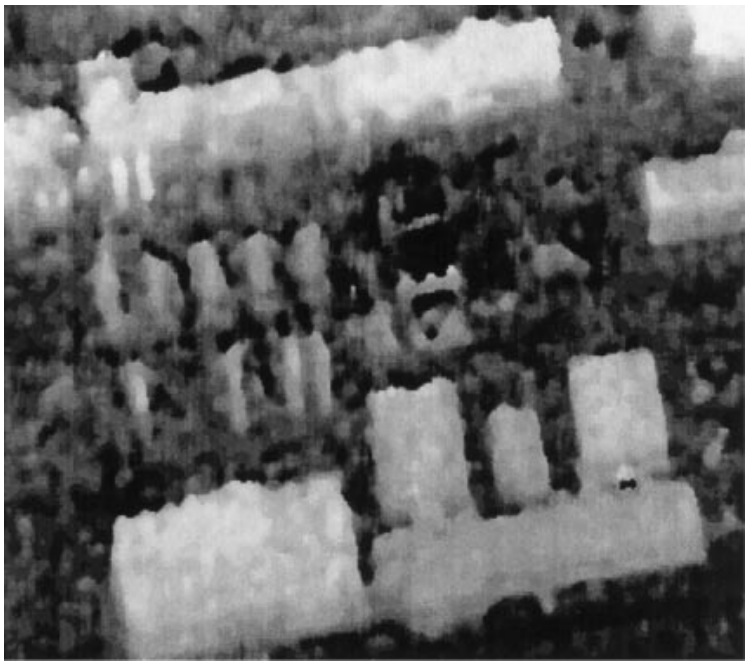

Fig. 3. An IFSAR image.

from IFSAR data: The data are noisy and the spatial resolution is much inferior to that of visual data. The spatial resolution is further degraded by the noise removal step. Figure 3 shows a height map produced by a real IFSAR. A typical IFSAR elevation image is noisy and needs to be filtered before it can be reliably used. Also, there are regions with "no data" that result either from the fact that the original scene was not on a rectangular grid or from radar geometry effects, which cause some points not to be mapped. Interpolation and nonlinear filtering techniques are used to filter the elevation data.

Positioning of IFSAR and visual data allows for the fusion of clues from both sensors for target recognition. It is needed to overcome various difficulties resulting from the limitations of the sensor. For example, building detection requires the extraction and grouping of features such as lines, corners, and building tops to form buildings (12). The features extracted from visual data usually contain many unwanted spurious edges, lines, and so on that do not correspond to buildings. The grouping stage requires complex and computationally intensive operations. Further, the height of a building is typically estimated by extracting shadows and sun angle when available and is not reliable when the shadows are cast on adjacent buildings. Another drawback of methods based exclusively on visual data lies in their sensitivity to imaging conditions.

IFSAR elevation data can be used in conjunction with visual data to overcome the aforementioned difficulties. Current IFSAR technology provides sufficient elevation resolution to discriminate building regions from surrounding clutter. These building regions are not well defined from a visual image when the buildings have the same intensity level as their surrounding background. Similarly, a building having different colors may be wrongly segmented into several buildings. IFSAR data are not affected by color variations in buildings and therefore are better for building detection.

Figure 4 shows a visual image and edges detected by the Canny operator for the area shown in Fig. 3. The top part of Fig. 4 shows a building with two different roof colors and roof structures on many buildings. Many spurious edges not corresponding to the building appear in the edge map shown on the bottom right of Fig. 4. Using the IFSAR elevation map shown in Fig. 3, buildings and ground regions are labeled using a two class

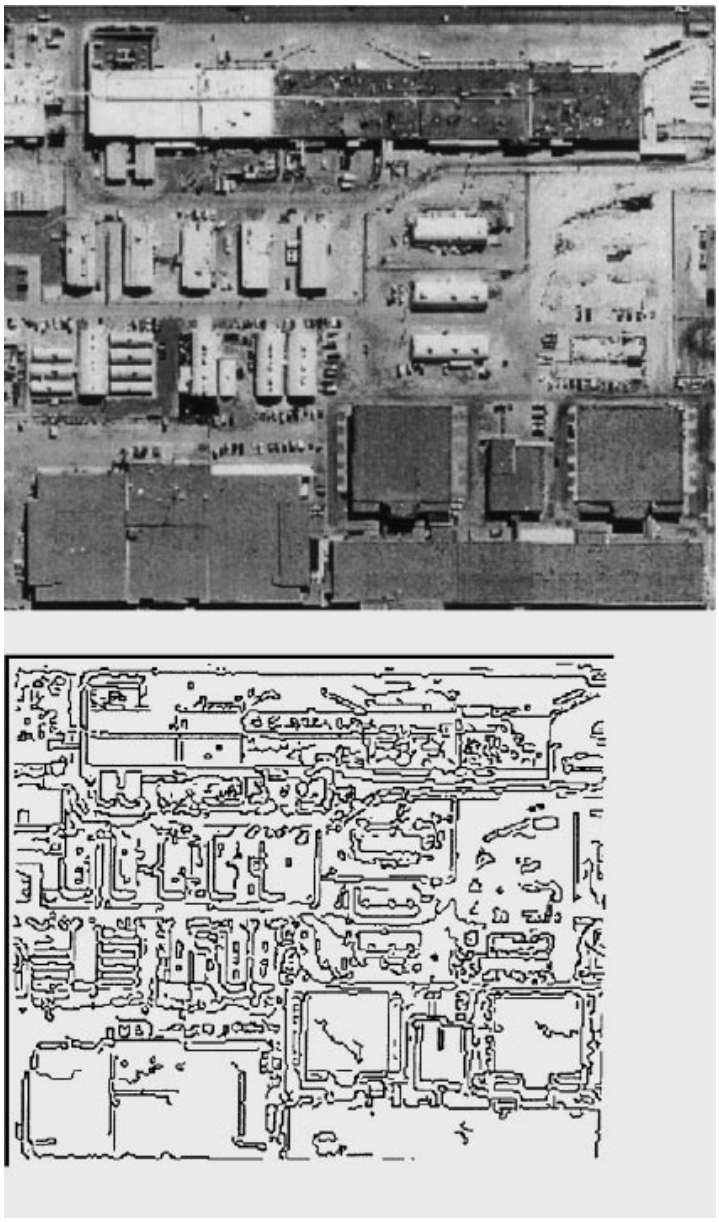

Fig. 4. Visual image and edges detected by the Canny operator.

classifier. The IFSAR and visual images are registered. Figure 5 shows the result of registration of a visual image and the segmented elevation image. Features corresponding to roads, parked cars, trees, and so on are suppressed from the visual images using the segmented buildings derived from the IFSAR image.

The locations and the directions of edges in the segmented image are estimated and are used to locate edges of buildings in the visual image. In the visual image, an edge pixel corresponding to each edge pixel in the registered height image is searched in the direction perpendicular to the estimated direction in the height

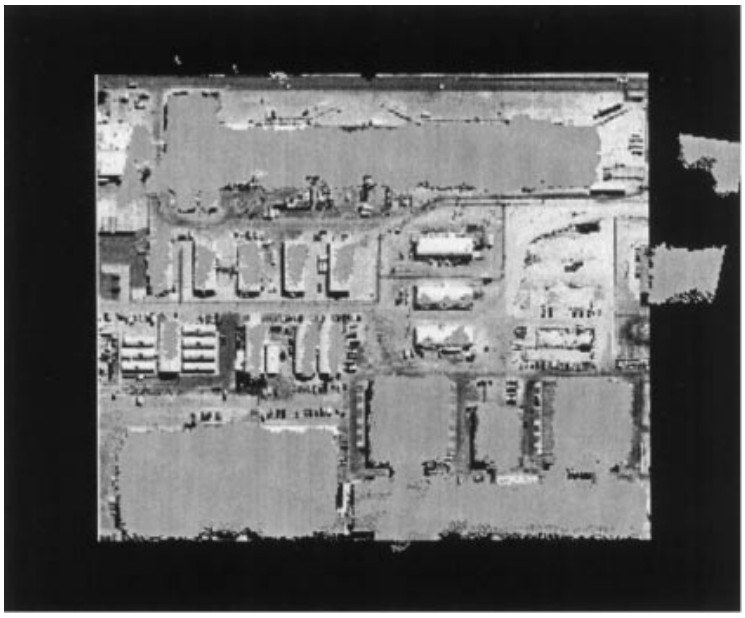

Fig. 5. Buildings segmented from the IFSAR image overlaid to visual image.

image. If an edge is found within a small neighborhood, the edge pixel is accepted as a valid edge of a building. If such a pixel is not found in the neighborhood, the edge is not accepted. Figure 6 shows the refined edges obtained by searching in the neighborhoods of height edges. Most of building edges in the height image are found while the unwanted edges are removed.

Spatial Matched Filter Classifiers for SAR (2)

A typical target recognition using SAR is done in multiple stages and is illustrated by the block diagram in Fig. 7 (13). In the first stage, a CFAR detector prescreens by locating potential targets on the basis of radar amplitude. Since a single target may produce multiple detections, the CFAR detections are clustered (grouped together). Then a region of interest (*ROI*) around the centroid of each cluster is passed to the next stage of the algorithm for further processing.

The second stage takes each ROI as its input and analyzes it. The goal of this discrimination stage is to reject natural-clutter false alarms while accepting real targets. This stage consists of three steps: (1) determining the position and orientation of the detected object, (2) computing simple texture features, and (3) combining the features into a discrimination statistic that measures how "targetlike" the detection object is.

The third stage is classification, where a 2-D pattern-matching algorithm is used to (1) reject clutter false alarms caused by man-made clutter discretes (buildings, bridges, etc.) and (2) classify the remaining detected objects. Those detected objects that pass the second stage are matched against stored reference templates of targets. If none of the matches exceeds a minimum required score, the detected object is classified as clutter; otherwise, the detected object is assigned to the class with the highest match score.

Matched filters are investigated in 2 as pattern-matching classifiers in the target recognition system shown in Fig. 7. They are synthetic discriminant function (*SDF*), the minimum average correlation energy (*MACE*) filter, the quadratic distance correlation classifier (*QDCC*), and the shift-invariant 2-D

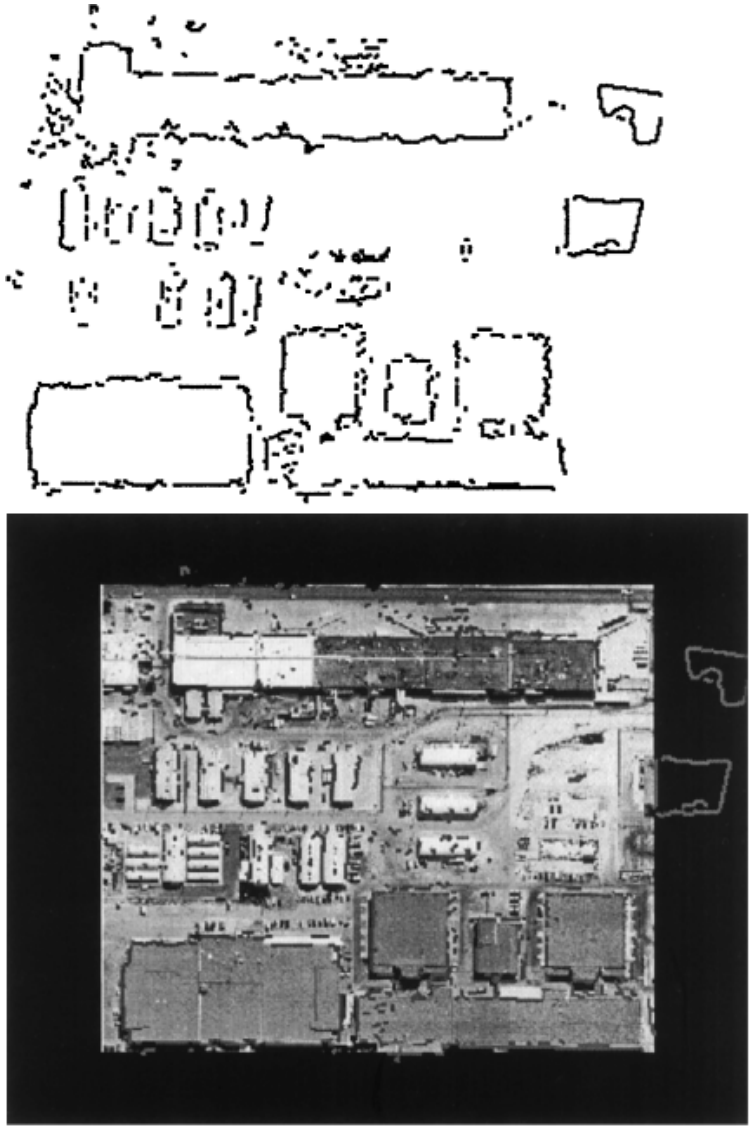

Fig. 6. Edges refined using IFSAR result.

pattern-matching classifier. The basic structure of the SDF and MACE filter is characterized in the frequency domain by

$$H = AX(X^{\dagger}AX)^{-1}U \tag{25}$$

where H denotes the DFT of the spatial matched filter. The matrix X is composed of a set of target training vectors obtained by taking the DFT of the target training images. The vector $\boldsymbol{U}$ represents a set of constraints imposed on the values of the correlation peaks obtained when the training vectors are run through the spatial matched filter. The matrix A represents a positive definite weighting matrix. A is an identity matrix for SDF

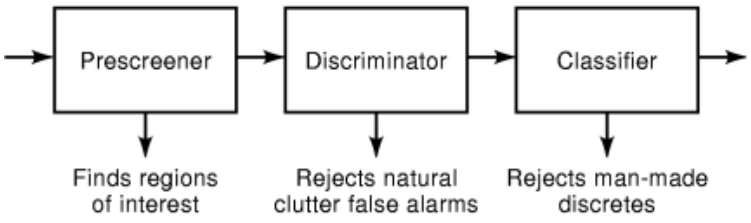

Fig. 7. Block diagram of a typical baseline target recognition system. [Adapted from Novak et al. (13)].

and is the inverse of the following matrix D.

$$D = \sum_{i=1}^{N} \text{diag}[|X_i(1)|^2, |X_i(2)|^2, \ldots, |X_i(p)|^2] \qquad (26)$$

where N is the number of training images and p is the dimension of the training vectors.

In the QDCC, the DFT of the spatial matched filter is expressed by

$$H = S^{-1}(m_1 - m_2) \qquad (27)$$

where m_1 and m_2 are means of the DFTs of the training images for classes 1 and 2, respectively. S is a diagonal matrix defined by

$$S = \frac{1}{N}\left[\sum_{i=1}^{N}(X_i - M_1)^{\dagger}(X_i - M_1) + \sum_{i=1}^{N}(Y_i - M_1)^{\dagger}(Y_i - M_1)\right] \qquad (28)$$

where M_1 and M_2 are matrices with elements of m_1 and m_2 placed on the main diagonal, and X_i and Y_i are ith training vectors from classes 1 and 2, respectively.

In the shift-invariant 2-D pattern-matching classifier, the correlation scores are calculated by

$$\rho_i = \max\{DFT^{-1}[R_i \times T^*]\} \qquad (29)$$

where T is the DFT of the dB-normalized test image and R_i is the ith reference template.

Novak et al. (2) did extensive experiment with the high-resolution (1 ft $\times$ 1 ft) fully polarimetric SAR data. In the four-class classification experiment using four types of spatial matched filter classifiers, it is reported that all targets are correctly classified (2).

Multisensor Fusion (8,14,15)

Research has been conducted on multisensor fusion for target recognition. Some of the motivating factors of such research are increased target illumination, increased coverage, and increased information for recognition. Significant improvement in target recognition performance has been reported (8) when multiple radar sources are utilized using sensor fusion approaches. Tenney and Sandell (14) developed a theory for obtaining the distributed Bayesian decision rules. Chair and Varshney (15) presented an optimal fusion structure given that

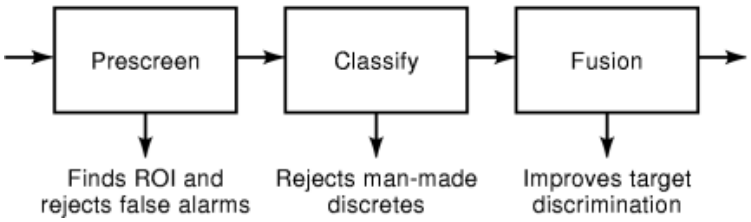

Fig. 8. A typical data fusion approach for target recognition. [Adapted from Heuter et al. (8)].

detectors are independently designed. The target recognition using multiple sensors is formulated as a two-stage decision problem in Ref. 8. A typical radar target recognition approach using data fusion is illustrated in Fig. 8. After the prescreening, single-source classifications are performed first; then the fusion of decision are performed.

The data fusion problem is treated as an m-hypothesis problem with individual source decisions being the observations. The decision rule for m-hypothesis is written as

$$\text{Decide } w_i \text{ if } g_i(u) > g_j(u) \text{ for all } j \neq i \tag{30}$$

For Bayes' rule, $g_i(u)$ is a posterior probability. That is,

$$g_i(u) = p(w_i|u) \tag{31}$$

Since the prior probability and the distribution of features cannot be estimated accurately, a heuristic function is used (8). It is a direct extension of Bayesian approach introduced by Varshney (16), and the function $g_i(\cdot)$ is generalized to include the full threshold range:

$$g_i(u) = \log \frac{P_1}{P_0} + \sum_{\Omega_1} \log \frac{P_i^d}{P_i^f} + \sum_{\Omega_0} \log \frac{1 - P_i^d}{1 - P_i^f} \tag{32}$$

where P_0 and P_1 are prior probabilities; Ω_1 and Ω_0 are the sets of all i such that $\{g_i(u) \geq T_i\}$ and $\{g_i(u) < T_i\}$, respectively, with T_i being the individual source threshold for partitioning decision regions; and the probabilities ${P^f}_i$ and ${P^d}_i$ are false alarm rates and probabilities of detections of each local sensor. The probabilities ${P^f}_i$ and ${P^d}_i$ are defined by the cumulative distribution functions (*CDF*) for each decision statistic. In practice, the CDFs are quantized and estimated from training on the individual sensor's classifier error probabilities. In a distributed scenario, the weighting can be computed at each sensor and transmitted to the fusion center, where they will be summed and compared to the decision threshold. In 8, the data fusion approach is applied to multiple polarimetric channels of a SAR image, and substantially improved classification performance is reported.

Summary

In radar target recognition, different types of radar are employed for different applications. In this article, radar target recognition approaches for different radar systems are discussed.

BIBLIOGRAPHY

1. A. W. Rihaczek, S. J. Hershkowitz, *Radar Resolution and Complex-Image Analysis*, Norwood, MA: Artech House, 1996.
2. L. M. Novak, Radar target identification using spatial matched filters, *Pattern Recognition*, **27** (4): 607–617, 1994.
3. J. D. Wald, D. B. Krig, T. DePersia, ATR: Problems and possibilities for the IU community, *Proc. ARPA Image Understanding Workshop*, January 1992, San Diego, CA, pp. 255–264.
4. M. W. Roth, Survey of neural network technology for automatic target recognition, *IEEE Trans. Neural Netw.*, **1**: 28–43, 1990.
5. A neural clustering approach for high resolution radar target classification, *Pattern Recognition*, **27** (4): 503–513, 1994.
6. L. I. Perlovsky *et al.*, Model-based neural network for target detection in SAR images, *IEEE Trans. Image Process.*, **6**: 203–216, 1997.
7. M. A. Rubin, Application of fuzzy ARTMAP and ART-EMAP to automatic target recognition using radar range profiles, *Neural Netw.*, **8**: 1109–1116, 1995.
8. A. Hauter, K. C. Chang, S. Karp, Polarimetric fusion for synthetic aperture radar target classification, *Pattern Recognition*, **30** (5): 769–775, 1997.
9. K. B. Eom, R. Chellappa, Non-cooperative target classification using hierarchical modeling of high range resolution radar signatures, *IEEE Trans. Signal Process.*, **45**: 2318–2327, 1997.
10. M. W. Roth, Neural networks for extraction of weak targets in high clutter environments, *IEEE Trans. Syst. Man Cybern.*, **19**: 1210–1217, 1989.
11. H. A. Zebker, R. M. Goldstein, Topographic mapping from interferometric synthetic aperture radar observations, *J. Geophys. Research*, **91**: 4993–4999, 1986.
12. R. Chellappa *et al.*, On the positioning of multisensor imagery for exploitation and target recognition, *Proc. IEEE*, **85**: 120–138, 1997.
13. L. M. Novak, A comparison of 1-D and 2-D algorithms for radar target classification, *Proc. IEEE Int. Conf. Syst. Eng.*, August 1991, pp. 6–12.
14. R. R. Tenney, N. R. Sandell, Detection with distributed sensors, *IEEE Trans. Aerosp. Electron. Syst.*, **17**: 501–510, 1981.
15. Z. Chair, P. K. Varshney, Optimal data fusion in multiple sensor detection systems, *IEEE Trans. Aerosp. Electron. Syst.*, **22**: 98–101, 1986.

READING LIST

J. S. Baras, S. I. Wolk, Model-based automatic target recognition from high-range-resolution radar returns, *SPIE Proc.*, **2234**: 57–66, 1994.

M. Basseville, A. Benveniste, A. S. Willsky, Multiscale autoregressive processes, Part I & II, *IEEE Trans. Signal Process.*, **40**: 1915–1954, 1992.

B. Bhanu, Automatic target recognition: State of the art survey, *IEEE Trans. Aerosp. Electron. Syst.*, **22**: 364–379, 1986.

V. Cantoni *et al.*, Recognizing 2D objects by a multi-resolution approach, *Proc. Int. Conf. Pattern Recognition*, Vol. 3, Jerusalem, Israel, October 1994, pp. 310–316.

N. C. Currie, R. D. Hayes, R. N. Trebits, *Millimeter-Wave Radar Clutter*, Norwood, MA: Artech House, 1992.

I. Daubechies, The wavelet transform, time-frequency localization and signal analysis, *IEEE Trans. Inf. Theory*, **36**: 961–1005, 1990.

D. M. Dunn, W. H. Williams, T. L. DeChaine, Aggregate versus subaggregate models in local area forecasting, *J. American Statistical Assoc.*, **71**: 68–71, 1976.

J. Geweke, Temporal aggregation in the multiple regression model, *Econometrica*, **46**: 643–662, 1978.

C. W. J. Granger, M. J. Morris, Time series modeling and interpretation, *J. Royal Statistical Soc.*, **A-139**: 246–257, 1976.

S. Kingsley, S. Quegan, *Understanding Radar Systems*, New York: McGraw-Hill, 1992.

D. C. McKee *et al.*, Model-based automatic target recognition using hierarchical foveal machine vision, *SPIE Proc.*, **2755**: 70–79, 1996.

R. A. Mitchell, R. Dewall, Overview of high range resolution radar target identification, *Proc. Automatic Target Recognition Working Group Conf.*, Monterey, CA, November 1994.

F. A. Pino, P. A. Morettin, R. P. Mentz, Modelling and forecasting linear combinations of time series, *Int. Statistical Rev.*, **55**: 295–313, 1987.
O. Rioul, A discrete-time multiresolution theory, *IEEE Trans. Acoust. Speech Signal Process.*, **41**: 2591–2606, 1993.
M. L. Skolink, *Introduction to Radar Systems*, New York: McGraw-Hill, 1980.
N. S. Subotic *et al.*, Multiresolution detection of coherent radar targets, *IEEE Trans. Image Process.*, **6**: 21–35, 1997.
L. G. Telser, Discrete samples and moving sums in stationary stochastic processes, *J. American Statistical Assoc.*, **62**: 484–499, 1967.
D. R. Wehner, *High Resolution Radar*, Norwood, MA: Artech House, 1987.
W. Wei, The effect of temporal aggregation of parameter estimation in distributed lag model, *J. Econometrics*, **8**: 237–246, 1978.
W. W. S. Wei, D. O. Stram, Disaggregation of time series models, *J. Royal Statistical Soc.*, **B-52**: 453–467, 1990.
M. A. Wincek, G. C. Reinsel, An exact likelihood estimation procedure for regression ARMA time series models with possibly non-consecutive data, *J. Royal Statistical Soc.*, **B-48**: 303–313, 1986.

KIE B. EOM
George Washington University